Journal of Power Sources 242 (2013) 638–645

Contents lists available at SciVerse ScienceDirect

Journal of Power Sources

journal homepage: www.elsevier.com/locate/jpowsour

# Microbial fuel cell with an algae-assisted cathode: A preliminary assessment

Araceli González del Campo [a], Pablo Cañizares [b], Manuel A. Rodrigo [b], Francisco J. Fernández [a], Justo Lobato [b,*]

[a] University of Castilla-La Mancha, Chemical Engineering Department, ITQUIMA, Av. Camilo José Cela S/N, 13071 Ciudad Real, Spain
[b] University of Castilla-La Mancha, Chemical Engineering Department, Building Enrique Costa Novella, Av. Camilo José Cela n° 12, 13071 Ciudad Real, Spain

## HIGHLIGHTS

- An MFC with not precious metal but using algae in the cathode has been implemented.
- At night the MFC still produces high amount of energy.
- The cathode has the biggest polarization resistance.
- Energy recovery from fruit juice industry wastewater has been produced.

## GRAPHICAL ABSTRACT

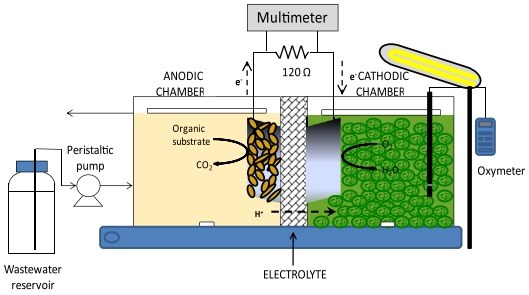


## ARTICLE INFO

*Article history:*
Received 14 December 2012
Received in revised form
29 April 2013
Accepted 23 May 2013
Available online 5 June 2013

*Keywords:*
Microbial fuel cell
Algae
$CO_2$
Acclimatization
Impedance
Polarization curve

## ABSTRACT

A microbial fuel cell (MFC) with an algae-assisted cathode, i.e., a system where the oxygen required by the cathode is not provided by aeration but by the photosynthetic process of the algae (*Chlorella vulgaris*), has been studied. The cathode was illuminated for 12 h each day (from 8:00 h to 20:00 h). 25 days was necessary to achieve steady state conditions. The time evolution of dissolved oxygen and cell voltage were assessed over the course of each day. As expected, the dissolved oxygen values were not constant throughout the day, reaching maximum values between 14:00 h and 20:00 h when dark phase reactions began and the algae started to consume oxygen. Cell voltage ($R_{ext}$ 120 Ω) followed the same trend as the oxygen profile. The supply of $CO_2$ in the cathode was also studied, and half an hour was enough time to get the system working properly. During the acclimation stage, power density increased up to 13.5 mW $m^{-2}$ at steady state conditions. However, impedance analysis showed that polarization resistance was higher at the cathode than at the anode. Nevertheless, it can be concluded that the studied system is a feasible method to treat wastewater in a self-sustainable way.



## 1. Introduction

The food products industry is very important in Spain, particularly in the region of Castilla-La Mancha. This industry comprises 16.38% of Gross National Product and has become one of the more healthy sectors of the Spanish economy.

Wastewater effluents from the fruit juice industry primarily contain high concentrations of organic materials (2300–11,000 mg $dm^{-3}$) [1], which are occasionally discharged into the municipal wastewater system and processed at wastewater treatment plants (WWTPs) with domestic wastewater. However, these effluents are usually pretreated in the factory prior to discharge in

* Corresponding author. Tel.: +34 926 29 5300; fax: +34 926295318.
*E-mail address:* Justo.lobato@uclm.es (J. Lobato).

0378-7753/$ – see front matter © 2013 Elsevier B.V. All rights reserved.
http://dx.doi.org/10.1016/j.jpowsour.2013.05.110

order to reduce their pollutant load. Due to the high solubility of pollutants and their high biodegradability, aerobic biological treatment is the preferred technology. Major problems associated to the treatment of raw effluent from the fruit juice industry include low pH values, unbalanced nutrient/COD ratios, and significant fluctuations in the daily profiles of flow and organic load [2,3]. In addition, aerobic biological treatment has some disadvantages, such as high sludge generation and high energy consumption. Thus, the aeration process is a predominantly energy-consuming process, comprising 30–55% of the total treatment energy demand [4] in aerobic biological treatment. Moreover, the costs of energy are rising as carbon-based resources become depleted and renewables struggle to make up the difference. Thus, a radical shift away from aerobic wastewater treatment technologies and toward an alternative that not only requires less energy but also produces energy is necessary to make the overall operation of wastewater treatment plants self-sustainable. Because the organic load of these effluents is not high enough for effective anaerobic treatment, alternative treatments have a great chance for development.

The microbial fuel cell (MFC) is a device that converts the chemical energy of a fuel (organic substrate) into electrical energy with the aid of biocatalytic reactions carried out by microorganisms [5]. Thus, MFCs provide new opportunities for the sustainable production of energy, in the form of electricity produced directly from biodegradable compounds. MFCs typically comprise an anode compartment and a cathode compartment separated by an ion-conducting membrane. In the anode compartment, microorganisms oxidize organic matter to carbon dioxide in anaerobic conditions and produce protons and electrons. Electrons pass through an external circuit, generating an electrical current. Protons cross the membrane to the cathode. In the cathode compartment, protons and electrons are combined with an electron acceptor, usually oxygen, to produce water.

Wastewater containing a high percentage of biodegradable organic compounds can be used as fuel in MFCs, achieving simultaneous wastewater treatment and energy production. Moreover, excess sludge production in an MFC is very low compared to conventional aerobic processes [6], which will help to minimize the overall operating cost of a treatment plant by decreasing the cost of sludge management.

Although MFCs are promising for wastewater treatment processes, there are still many technical and economic obstacles to overcome before practical applications will be feasible [7]. Currently, platinum is often used to catalyze oxygen reduction, which requires a significant investment cost. For this reason, some researchers have recently started working on the concept of biocathodes. There are three different concepts:

i) Aerobic biocathodes that use oxygen as the oxidant and microorganisms to assist the oxidation of transition metal compounds, such as Mn(II) or Fe(II), for electron delivery to oxygen [8].
ii) Anaerobic biocathodes that use compounds such as nitrate, sulfate, iron, manganese, selenate, arsenate, urinate fumarate and carbon dioxide as terminal electron acceptors [9].
iii) Algal biocathodes in which the cost of aeration is reduced by changing the mechanical aeration device to an algal oxygen supply, which can also reduce $CO_2$ emissions from the factory [10,11]. Hence, a photosynthetic culture of algae at the cathode, with light radiation, utilizes $CO_2$ as the carbon source for photosynthesis and produces oxygen, which acts as an electron acceptor for electricity generation. Algae can also act as a biological electron acceptor while simultaneously reducing carbon dioxide to biomass [12].

These systems represent the first approach to designing a lagooning wastewater treatment process with microbial fuel cells [13] for the treatment of wastewater from the fruit juice industry.

The aim of this work was to assess the start-up of a microbial fuel cell fed with synthetic fruit juice waste, where the cell was equipped with an algae-assisted cathode with the aim of producing oxygen at a low cost. The use of algae at the cathode has advantages that include eliminating the need for a mechanical air supply at the cathode (with corresponding cost savings) and reducing the $CO_2$ emitted from bacterial respiration and metabolism. Furthermore, in our system, no external mediators or precious catalysts were necessary.

## 2. Materials and methods

### 2.1. Experimental set-up

The set-up used in this study, Fig. 1, consisted of a two-chambered (800 $cm^3$ each) MFC, using a proton exchange membrane (PEM, by Sterion®) with high ion exchange capacity (0.9–0.02 meq $g^{-1}$), high ionic conductivity ($8 \cdot 10^{-2}$ S $cm^{-1}$) and low electronic conductivity ($<10^{-10}$ S $cm^{-1}$) to separate the electrodes. Both electrodes were built of Toray carbon cloths with 10% Teflon to improve the mechanical properties of the carbon support over the course of the study and because Teflon only caused a small drop in performance [14]. The active area of each electrode was 8 $cm^2$. Both electrodes were connected by an external resistance ($R_{ext}$) of 120 Ω; this low value was chosen to prevent activation losses and facilitate electron transfer during the acclimation period [15].

### 2.2. Inoculum

Activated sludge from a wastewater treatment plant (Ciudad Real, Spain) was used as the inoculum for the anodic compartment; it was fed in batch mode with a synthetic fruit processing industry effluent containing 322 mg $dm^{-3}$ of sugar (fructose and glucose) and nutrients as shown in Table 1. This composition is very similar to the composition of wastewater from the fruit juice industry, taking into account the organic composition of fruit juice [16]. First, activated sludge was introduced into the anodic compartment with synthetic wastewater in a 3:1 ratio. The anode chamber was covered from light to prevent the growth of algae [15].

The cathode compartment contained a culture of *Chlorella vulgaris*. This compartment was illuminated for 12 h a day (from 8:00 h to 20:00 h) with an 11 W fluorescent lamp (Philips) located 10 cm above the reactor, and it was controlled by means of a programmable timer (Noru). Hence, the MFC was operated under a 12 h light and 12 h dark regime. Every day, water evaporated from the

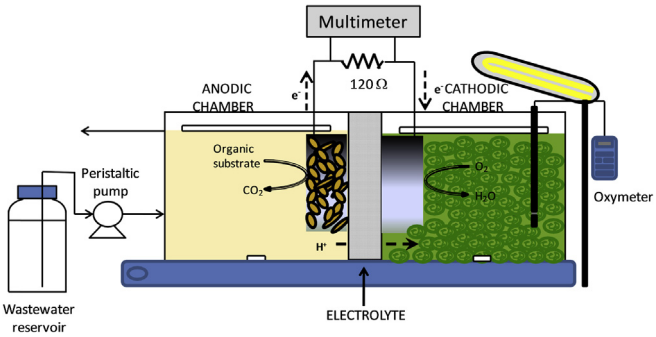


**Fig. 1.** Schematic view of the set-up.

**Table 1**
Characteristics of the synthetic wastewater.

| Component | Concentration (mg dm$^{-3}$) |
|---|---|
| Fructose | 161 |
| Glucose | 161 |
| $NaHCO_3$ | 111 |
| $(NH_4)_2SO_4$ | 74.2 |
| $KH_2PO_4$ | 44.5 |
| $MgCl_2$ | 37.1 |
| $CaCl_2$ | 30.7 |
| $(NH_4)_2 \cdot Fe(SO_4)_2$ | 3.1 |

cathodic chamber was replenished with Bold's basal medium [17] and $CO_2$ was bubbled. The temperature in both compartments was 26 ± 1 °C.

The overall biochemical reactions that occurred at the anode and cathode chambers of the MFCs were as follows [18]:

Anode chamber:

$$C_6H_{12}O_6 + 6H_2O \rightarrow 6CO_2 + 24H^+ + 24e^- \quad (1)$$

Cathode chamber (during the light period):

$$nCO_2 + nH_2O \overset{(\text{algae}+h\nu)}{\rightarrow} (CH_2O)_n(\text{biomass}) + nO_2 \quad (2)$$

$$O_2 + 4e^- + 4H^+ \rightarrow H_2O \quad (3)$$

During the light period, algae carry out photosynthesis, using carbon dioxide and light to produce organic matter and biomass. During the dark period, algae consume oxygen to oxidize the organic matter previously created to obtain energy, according to reaction (4) [19]:

$$C_6H_{12}O_6 + 6O_2 \rightarrow 6CO_2 + 6H_2O \quad (4)$$

In this way, during the dark period, oxygen is consumed by the respiration of algae and reduction reactions which take place in the cathodic chamber.

### 2.3. Analysis

A digital multimeter (Keithley 2000 multimeter) was used to continuously monitor the cell voltage at the value of the external load (120 Ω). Dissolved oxygen of the cathodic compartment was continuously monitored with an Oxi538 WTW oxymeter. At both compartments, conductivity was measured with a Jenway 470 conductivity meter and pH and redox potential were measured with a PCE-228 pH meter. Volatile suspended solids were measured according to APHA (1998) [20]. The COD was determined by photometric methods with a MERCK COD cell test and Pharo 100 MERCK spectrophotometer.

An Autolab PGSTAT30 potentiostat/galvanostat (Ecochemie, The Netherlands) was used to record polarization curves and perform electrochemical impedance spectroscopy (EIS). Polarization curves were recorded to determine the following: the open circuit voltage (OCV) or the maximum allowable MFC voltage (for a nil current), the maximum power density, the current density at the maximum power density and the internal resistance. A scan rate of 1 mV s$^{-1}$ and a step potential of 1 mV were used. The internal resistance, $R_{int}$ (Ω), was calculated according to the following Eq. (5):

$$R_{int} = \frac{P_{max}}{I^2_{P_{max}}} \quad (5)$$

To quantify and analyze the ohmic (or diffusion) and the polarization (or charge transfer) resistance, impedance spectroscopy was carried out. EIS measurements were carried out under open circuit conditions using the frequency response analyzer (FRA) module. The frequency of the AC signal was varied from 10 kHz to 1 mHz with an amplitude of 10% of OCV. The EIS were taken on two different design configurations: complete cell and anode. The complete cell EIS measurements were performed using the cathode as the working electrode, while the anode was used as a counter and reference electrode. The anode EIS measurements were performed by placing an SCE reference electrode in the anode compartment, while the working electrode was the anode and the counter electrode was the cathode [21].

## 3. Results and discussion

### 3.1. Acclimatization of the microorganisms

As in any biological process, for the start-up of an MFC, the acclimation of microorganisms is a necessary first step. To do that, activated sludge from an urban WWTP was used to inoculate the anode chamber of the MFC, which was loaded with synthetic fruit juice industry wastewater at a ratio of 3:1 (v/v). The mixture was kept under anaerobic conditions for days (acclimation period) to allow electricity-producing microorganisms (EPM) to grow. At the cathodic compartment, a culture of algae obtained from the cathode of another algal fuel cell was seeded to reach a concentration of approximately 300 mg dm$^{-3}$. Thus, no acclimation of these algae was required. As will be described, the continuous production of electricity marked the end of the acclimation period.

During the acclimation stage, the MFC was operated in semi-continuous mode with a short sludge age of 8 days. To attain these conditions, 100 cm$^3$ of mixed liquor were purged daily from the anodic compartment and replaced by synthetic wastewater. It was expected that this high purge rate would force the EPM to form a biofilm on the anode.

In Fig. 2A, the changes in cell voltage (external resistance of 120 Ω) during acclimation are shown. As expected, the cell voltage was low during the first 5 days, indicating that EPM were not the predominant microorganisms in the seeded sludge. However, a very interesting observation was the production of bioelectricity from the beginning, suggesting that some EPM were present in the seeded sludge and produced energy even in this lag stage. After 5 days, cell voltage increased, marking an exponential growth stage. Then, after approximately 25 days, the system reached a steady state characterized by a constant cell voltage of approximately 18 mV ($R_{ext}$ = 120 Ω). This result is in agreement with recent works on MFCs, in which values of 20–30 days to reach a steady state have been reported [15]. More recently, our group has reported values of 15 days to reach steady state conditions using the same cathode-assisted microbial fuel cell but loaded with wastewater of a different composition and operated continuously [13].

During the acclimation of microorganisms, other important parameters for the operation of an MFC, such as pH, conductivity, redox potential, COD removal, microorganisms and algae concentration, were monitored. However, only those parameters showing a significant influence on the results are discussed here.

The electrolyte pH could play an important role on the efficiency of MFCs. It is known that pH is an important parameter for microorganisms and algae because they can only carry out their vital functions across a limited pH range. For this reason, most MFCs are operated at neutral pH to optimize bacterial and algal growth conditions. With regard to the anode, the pH can influence aerobic metabolic activity and in turn affect electron and proton generation mechanisms [22]. Values outside the 6.5–8.5 range are known to

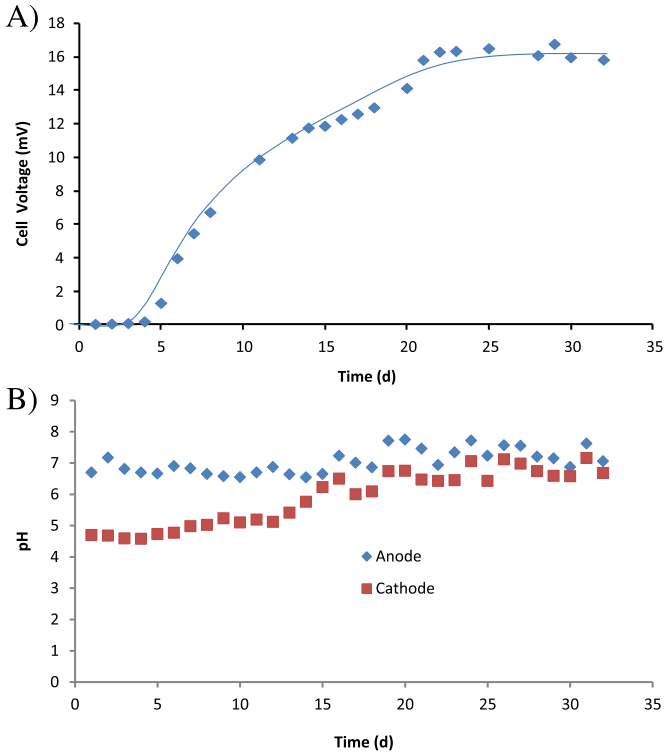


**Fig. 2.** Evolution of cell voltage and pH at the anodic and cathodic compartments during the acclimatization stage of the microorganisms. (A) Cell voltage. (B) pH.

strongly disfavor microorganism metabolism. Regarding the cathode, *Chlorella* sp. is reported to grow optimally at pH values that range from 7.5 to 8.0 [23,24]. Acidic (in the range 3.0–6.2) and alkaline (in the range 8.3–9.0) values are known to retard the growth of this alga [23], although their activity is not entirely stopped. Outside of the proposed ranges, algal activity is not observed. Hence, it is important to maintain a neutral or lower pH near the cathode to maximize power generation [25]. However, a low concentration of protons at roughly neutral pH makes the internal resistance of the cell relatively high, especially if compared to that of conventional chemical PEM fuel cells that use acidic electrolytes.

In Fig. 2B, the changes in the anode and cathode pH can be observed. The pH of the anode during the acclimation stage remained approximately constant at 7.0, despite the development of an EPM culture during this period (only a small increase was observed). This finding means that no significant biological processes that affect pH such as acidogenic fermentations occur [26]. In contrast, the pH of the cathode increased slowly from 5.0 to 7.0; the buffering effect of carbonates/bicarbonates may explain this observation.

Another important parameter is the concentration of microorganisms and algae in the anodic and cathodic compartments; these results are shown in Fig. 3. At the beginning of the experiment, just after seeding the compartments, microorganism concentrations were as high as 2150 mg $dm^{-3}$, but microorganism concentrations decreased during acclimation to approximately 100 mg $dm^{-3}$. This decrease can be attributed to the short sludge age used, which promoted only the growth of EPM in a biofilm on the anode surface and decreased the concentration of microorganisms in suspension (i.e., microorganism washing) [13].

The algae concentration decreased during the first 10 days and then returned to the initial concentration. The effect of pH on algal activity could explain this behavior because algal activity is promoted within the range of 7.5–8.0, as shown in Fig. 2B. Algae are

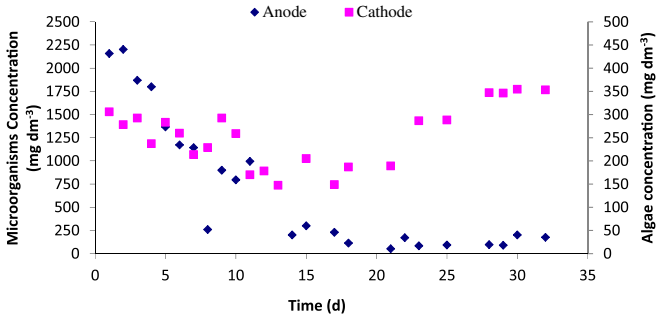


**Fig. 3.** Evolution of microorganisms and algae concentrations during acclimation of the microorganisms.

autotrophic microorganisms that do not need to consume other microorganisms for food. Thus, algal concentrations should increase, but this was not observed because other heterotrophic microorganisms grew in the cathode and consumed the dead algae. However, this phenomenon did not affect the efficiency of the fuel cell because, during the day, dissolved oxygen concentrations reached the oxygen saturation point.

An important parameter in this type of bioelectricity generating system is the COD removal rate. This parameter was estimated every day and is shown in Fig. 4. During the first days (corresponding to the lag stage of EPM), both the COD removal efficiency and rate were high, with values approximately 80% and 16.0 mg $dm^{-3}$ $h^{-1}$, respectively. Seed sludge came from a municipal WWTP (where it was acclimated to a more complex wastewater) and the concentration of sludge was very high (indicating a high concentration of active microorganisms). Both factors explain the good performance of the biological system in the removal of pollution. Then, a low oxygen concentration in the anodic chamber with a short sludge age promoted the washing out of aerobic microorganisms and the prevalence of EPM (exponential stage described for Fig. 2). As the total concentration of microorganisms decreased, the rates and efficiencies of COD removal decreased as well, down to the ranges of 46–60% and 6.5–8.0 mg $dm^{-3}$ $h^{-1}$ for COD removal efficiency and rate, respectively. These values are similar to the ones obtained by Ahn and Logan [27], who studied domestic wastewater treatment using microbial fuel cells at different temperatures, where COD degradation rates were 9 mg $dm^{-3}$ $h^{-1}$ for mesophilic and 11 mg $dm^{-3}$ $h^{-1}$ for ambient conditions.

Fig. 5 shows the dissolved oxygen in the cathodic compartment and the cell voltage ($R_{ext}$ = 120 Ω) at every hour during one day, once the MFC reached steady state conditions. At 8:00 h, when the light was switched on, the illumination phase started and algae carried out photosynthesis, capturing light and carbon dioxide and

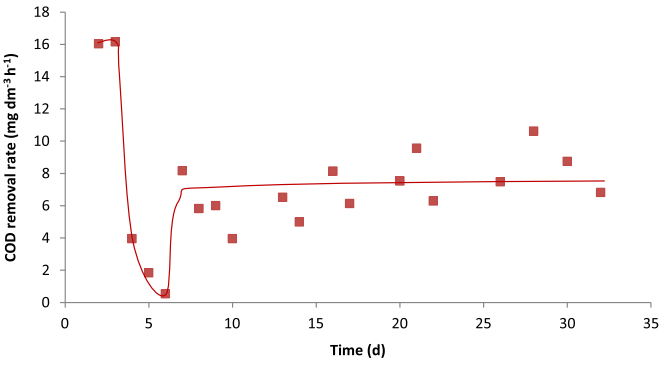


**Fig. 4.** Evolution of the COD removal rate during acclimation of the microorganisms.

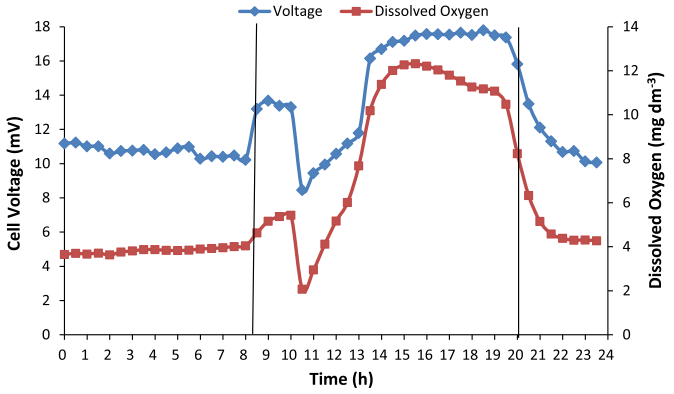


**Fig. 5.** Evolution of cell voltage and dissolved oxygen during one day.

releasing oxygen. Thus, it can be observed that dissolved oxygen at the cathode increased and cell voltage also increased. At 9:00 h, dissolved oxygen at the cathode and cell voltage decreased to 2 mg $dm^{-3}$ and 8 mV ($R_{ext}$ = 120 Ω), respectively, because as the carbon dioxide necessary for photosynthesis was bubbled into the cathodic compartment, the displacement of oxygen could occur, which would contribute to decreased cell voltage. Afterwards, cell voltage and dissolved oxygen increased until steady state values were reached at 14:00 h. These values were constant at approximately 18 mV ($R_{ext}$ = 120 Ω) and 12 mg $dm^{-3}$, respectively, until 20:00 h, when the light was switched off and the dark phase began. During the dark phase, algae consumed oxygen by respiration. At this point, dissolved oxygen and the cell voltage fell to 4 mg $dm^{-3}$ and 11 mV ($R_{ext}$ = 120 Ω) at 23:00 h, respectively. These results suggest that oxygen concentrations at the cathode control the overall MFC performance under our operation conditions. This effect was also observed by Strik D.P.B.T.B. et al. [28], who studied a solar energy powered microbial fuel cell [28]. Hence, a close relationship between dissolved oxygen in the cathode and cell voltage can be observed. This behavior has also been observed in a standard MFC [14], where dissolved oxygen had a significant influence on MFC performance. Nevertheless, our algae-assisted MFC still produced energy during the dark phase, at more the 60% of the values observed during the light phase. It is not easy to explain this behavior, but it is known that in previous works [29], under low oxygen concentrations, substances other than oxygen have acted as electron acceptors. Recent studies in our lab are verifying this phenomenon, but further studies are being developed to help us understand the behavior of our MFC during the dark period.

During the acclimation period, conductivity and redox potential were also measured every day. Conductivity of the cathode was constant with a value of 1200 μS $cm^{-2}$. However, conductivity of the anode decreased from 1500 to 700 μS $cm^{-2}$. This is simply because the seeded activated sludge had a higher conductivity than the synthetic wastewater fed into the system. In the anodic compartment, the redox potential was maintained at a value constant of −50 mV. Whereas in the cathodic compartment, the redox potential varied throughout the day according to the concentration of dissolved oxygen. In the morning and at night, when oxygen dissolved in the cathode was lowest, the redox potential was close to −50 mV, and in the afternoon, when the dissolved cathode oxygen was its highest, the redox potential increased up to 20 mV.

### 3.2. Study of the addition of $CO_2$

Algae are autotrophic photosynthetic organisms that use carbon dioxide as a carbon source for growth. As explained in the Experimental section, to provide this carbon source, $CO_2$ was bubbled through the system every day to simulate the absorption of carbon dioxide emissions from a plant (mainly associated with the heat required for evaporators). In order to optimize the $CO_2$ dose, a preliminary study was undertaken, in which $CO_2$ was bubbled at the cathode for 0.5 h–1.0 h on different days and the results were compared with those obtained when $CO_2$ was not added. The intention was to determine if a continuous supply of carbon dioxide was necessary for algal growth or if their requirements are small enough that hourly dosing could fulfill their carbon needs.

In Fig. 6A and B, the profiles of cell voltage ($R_{ext}$ = 120 Ω) and dissolved oxygen are shown during days when $CO_2$ was bubbled for 0.5 h and 1.0 h and when $CO_2$ was not bubbled. When $CO_2$ was bubbled, decreases in dissolved oxygen and cell voltage were observed, which could be due to the stripping of oxygen from the water. Less oxygen was stripped when $CO_2$ was bubbled for only 0.5 h, so the MFC recovered more quickly, reaching its maximum steady state value again after 1.0 h. However, when $CO_2$ was bubbled for 1.0 h, 4.0 h was needed for cell performance to recover. When $CO_2$ was not added, the maximum cell voltage was lower, indicating that in this case, the oxygen profile was not disturbed. In addition, changes in cell voltage and dissolved oxygen during the day can be seen in Fig. 6C. The first day, $CO_2$ was bubbled for 0.5 h and on the following days, $CO_2$ was not added. Thus, dissolved oxygen was constant at approximately 6.0 mg $dm^{-3}$ every day. However, cell voltage did decrease with time, from 17 mV ($R_{ext}$ = 120 Ω) to 14 mV ($R_{ext}$ = 120 Ω). This change allowed us to conclude that the addition of carbon dioxide was necessary to assure good algal performance.

For this system, $CO_2$ bubbled for 0.5 h was enough to achieve a good response in the algal MFC. In other words, benefits were not observed if more $CO_2$ was bubbled into the cathode because the carbon requirements were completed within this 0.5 h period. This indicates that there is a limit to the amount of carbon dioxide that can be stored with this technique, and adding more than this amount does not improve performance.

### 3.3. Electrochemical characterization during acclimatization

During the acclimation of microorganisms, electrochemical characterization was carried out. Polarization curves were measured on the 5th, 10th, 13th, 20th, 24th and 27th days. Table 2 shows electrochemical parameters obtained from the polarization curves, such as the maximum power density (mW $m^{-2}$), the current density obtained at maximum power density (mA $m^{-2}$), the internal resistance (kΩ) and the OCV (mV). It can be seen that the maximum power density and current density increased from 3.63 to 14.40 mW $m^{-2}$ and from 25.09 to 116.96 mA $m^{-2}$, respectively, because EPMs grew and adapted to the conditions, hence producing more electricity. The internal resistance decreased during acclimation from 7.2 to 1.3 kΩ, and therefore, ionic and electrical conductivity improved. In this way, the maximum power density was 14.40 mW $m^{-2}$ and the minimum internal resistance was 1.3 kΩ.

In this way, the maximum power density obtained was similar to or higher than that published by other authors for conventional MFCs where catalysts were not used [5,31–32]. Thus, Kim et al. [30] studied an MFC operated in batch mode, without a catalyst in the cathode and using an enriched microbial consortium in the anode; in this study, a maximum power density of 8.3 mW $m^{-2}$ was obtained. In a study on electricity generation by *Geobacter sulfurreducens* in an unmediated MFC, which was operated in batch mode without a cathodic catalyst and carried out by Bond and Lovley [31], a maximum power density of 16 mW $m^{-2}$ was obtained. This value was higher than the maximum power density of the present study because a pure culture was used as the biocatalyst in the anode. Moreover, the maximum power density obtained in this study is higher than in others

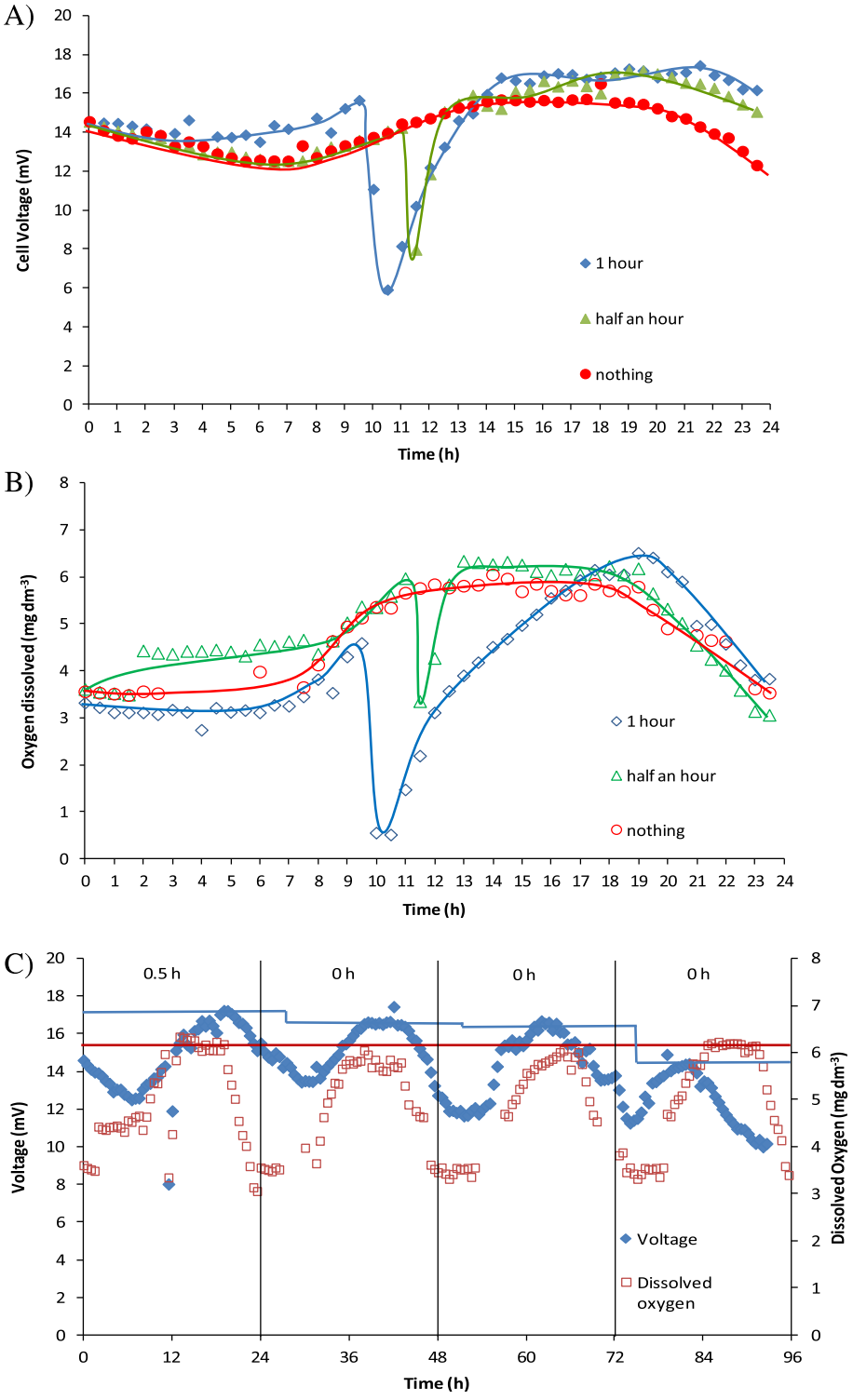


**Fig. 6.** Evolution of voltage and dissolved oxygen with and without the addition of $CO_2$. (A) Cell voltage. (B) Dissolved oxygen. (C) Dissolved oxygen and cell voltage during different days with and without the addition of $CO_2$.

published on photo-microbial fuel cells similar to those used in this study [33]. For example, Powell et al. [12] reached a maximum power density of 2.7 mW $m^{-2}$ with *C. vulgaris* at the cathode.

Thereby, photo-microbial fuel cells without catalysts showed a maximum power density of 0.82 mW $m^{-2}$ [31]. In contrast, in microbial fuel cells where a white-rot fungus was used as a bio-cathode and platinum was used as a catalyst, Wu et al. [34] obtained a maximum power density of 6.4 mW $m^{-2}$. With respect to the OCV values, these were constant across every day and similar to values published by Ieropoulos et al., where a large (500 $cm^3$) unit MFC was studied [35].

Electrochemical impedance spectroscopy was carried out on the 10th, 17th, 25th and 32nd days with two different configurations, designated complete cell and anode. The equivalent electrical

**Table 2**
Electrochemical parameters obtained during the acclimation stage from polarization curves.

| Day | $P_{max}$ (mW m$^{-2}$) | $I_{max}$ (mA m$^{-2}$) | OCV (mV) | $R_{int}$ (kΩ) |
|---|---|---|---|---|
| 5 | 3.63 | 25.09 | 479.9 | 7.2 |
| 10 | 9.73 | 72.79 | 490.4 | 2.3 |
| 13 | 13.53 | 104.25 | 489 | 1.6 |
| 20 | 14.40 | 116.96 | 462.8 | 1.3 |
| 24 | 12.35 | 93.72 | 460.8 | 1.8 |
| 27 | 13.16 | 93.69 | 459.9 | 1.9 |

**Table 3**
Parameters from equivalent circuit fitting of the complete cell and anode impedance data.

| Day | $R_{ohm}$ (Ω) | $R_{pol}$ complete cell (Ω) | $R_{pol}$ anode (Ω) |
|---|---|---|---|
| 10 | 1441.0 | 145,000 | 1069 |
| 17 | 3230.0 | 58,600 | 1362 |
| 25 | 217.9 | 22,670 | 1002 |
| 32 | 192.8 | 17,690 | 938 |

circuit, shown in Fig. 7A, was used to fit the impedance data to obtain the ohmic and polarization resistances. The equivalent circuit model consisted of an ohmic resistance component (related to membrane + solution resistance), followed by polarization resistance component (related to charge transfer between anode and cathode and surrounding electrolyte/bacteria–alga), which is in parallel with a constant phase element (CPE).

The CPE is used in the place of a capacitor to simulate the non-ideal behavior of distributed capacitance, typical of porous electrodes [36]. In Fig. 7B and C, Nyquist plots of the complete cell at different days can be observed. Impedance spectra show a high polarization resistance represented by an unclosed semicircle for the complete cell and a closed semicircle for the anode (representation not shown). The first intersection of the Nyquist plot with the *x*-axis represents the solution + membrane resistance (ohmic resistance). The projected point of the intersection curve with the *x*-axis farthest from the origin is representative of the total impedance [37]. Table 3 shows the parameter from the equivalent circuit fitting the complete cell and anode EIS data. The correlation coefficient was 0.98 in all cases. The ohmic resistance of the MFC decreased during acclimatization from 1441 to 192.8 Ω, and complete cell polarization resistance decreased from 145,000 to 17,690 Ω.

From electrochemical impedance spectroscopy of the anode compartment, the anode polarization resistance was also calculated. Thus, this value decreases from 1069 to 938.3 Ω, which indicated that the polarization resistance of the anodic compartment is much lower than the polarization resistance of the cathodic compartment. Therefore, the high polarization resistance of the complete microbial fuel cell was due to the high polarization resistance of the cathode. The values of anode polarization resistance were lower than the

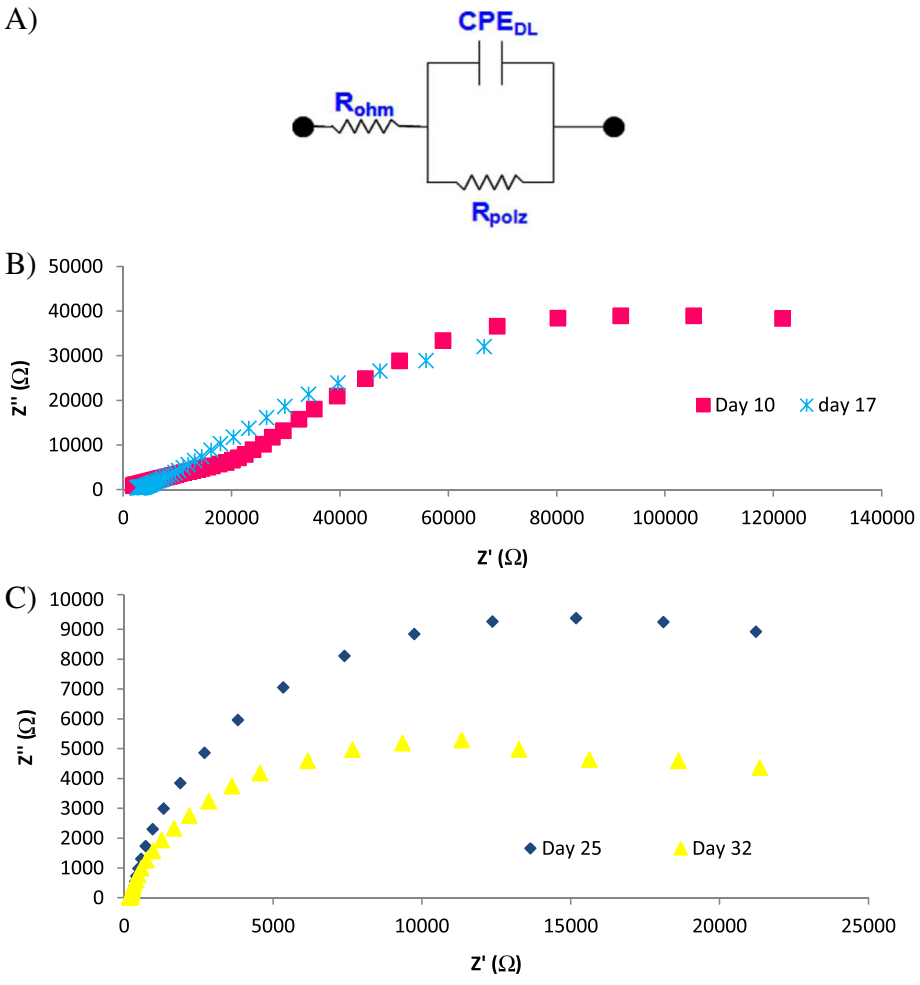


**Fig. 7.** Impedance analysis of the microbial fuel cell. (A) Equivalent circuit. (B) Nyquist plots of days 10 and 17. (C) Nyquist plots of days 25 and 32.

values obtained in other research; however, the values of complete cell polarization resistance were higher than the values obtained in other studies [21,38,39]. The cathode polarization resistance was higher than the anode polarization resistance because, in this set-up, a precious catalyst was not used in the cathode.

In this way, Ramasamy et al. [21] performed EIS experiments during the biofilm growth on the anode of an MFC, and impedance measurements were taken on three different configurations designated the complete cell, anode and cathode. The electrochemical polarization resistances of the complete cell and anode on day 1 were estimated to be 40,050 Ω and 39,150 Ω, respectively. For the MFC with the established biofilm, this value was 8250 Ω and 7200 Ω for the complete cell and anode, respectively. In another study by Manohar et al. [39], impedances were carried out on three different configurations: complete cell, anode and cathode. A buffer was used to control the pH, and lactate and *Shewanella oneidensis* were used as analytes. In this case, the polarization resistances of the complete cell and anode were 72,000 Ω and 10,200 Ω, respectively.

Although neither of our electrodes used catalysts, one must remember that a biofilm formed on the surface of the anode, which acted as a biocatalyst for the anodic reactions [40], whereas on the cathode surface, an active biofilm was not formed. In this system, the algae mainly acted as oxygen producers (during the radiation period) not as oxygen reducers, which could explain why, in all cases in our study, the cathode was the limiting electrode for high power output.

## 4. Conclusions

The feasibility of a microbial fuel cell with an algae-assisted cathode has been demonstrated to treat synthetic fruit juice production effluent and to simultaneously produce electricity. The algae were able to produce the oxygen required for the system under our operating conditions. The time required for the acclimation stage was similar to that for standard microbial fuel cells. The production of electricity was not constant, depending on the oxygen concentration, which depended on the time length of illumination. This technology was also able to produce a great amount of electricity during the dark phase (at night). Bubbling $CO_2$ into the cathode, for 30 min each day, was enough time for the efficient operation of the MFC. Finally, it can be concluded that the polarization resistance of the cathode was higher than the polarization resistance of the anode and that cathodic reactions were the limiting steps in this technology.

Further research in our lab is aimed at improving the performance of this photosynthetic system coupled with the MFC and toward a better understanding of this technology.

## Acknowledgments

The authors thank JCCM for financial support thorough the Project POII10-0329-5194.

## References

[1] H. El-Kamah, A. Tawfik, M. Mahmoud, H. Abdel-Halim, Desalination 253 (2010) 158–163.
[2] U. Austerman-Haun, C.F. Seyfried, K.-H. Rosenwinkel, Water Sci. Technol. 36 (1997) 407–414.
[3] P.L. Dold, G.A. Ekama, G.V.R. Marais, Water Technol. 12 (1980) 47–77.
[4] EPA, Water and Energy: Leveraging Voluntary Programs to Save Both Water and Energy, Environmental Protection Agency, 2008.
[5] H.J. Kim, H.S. Park, M.S. Hyun, I.S. Chang, M. Kim, B.H. Kim, Enzyme Microb. Technol. 30 (2002) 145–152.
[6] K. Rabaey, G. Lissens, S.D. Siciliano, W. Verstraete, Biotechnol. Lett. 25 (2003) 1531–1535.
[7] A.E. Franks, K.P. Nevin, Energies 3 (2010) 899–919.
[8] P. Clauwaert, D. Van der Ha, N. Boon, K. Verbeken, M. Verhaege, K. Rabaey, Environ. Sci. Technol. 41 (2007) 7564–7569.
[9] Z. Hu, J. Power Sources 179 (2008) 27–33.
[10] S. Freguia, K. Rabaey, Z.G. Yuan, J. Keller, Environ. Sci. Technol. 41 (2007) 2915–2921.
[11] S. Solomon, G.K. Plattner, R. Knutti, P. Friedlingstein, Proc. Natl. Acad. Sci. U S A 106 (2009) 1704–1709.
[12] E.E. Powell, M.L. Mapiour, R.W. Evitts, A.H. Gordon, Bioresour. Technol. 100 (2009) 269–274.
[13] J. Lobato, A. Gonzalez del Campo, F.J. Fernandez, P. Cañizares, M.A. Rodrigo, Appl. Energy. 110 (2013) 220–226.
[14] J. Lobato, P. Cañizares, M.A. Rodrigo, C. Ruiz-López, J.J. Linares, J. Appl. Electrochem. 38 (2008) 793–802.
[15] M.A. Rodrigo, P. Cañizares, H. García, J.J. Linares, J. Lobato, Bioresour. Technol. 100 (2009) 4704–4710.
[16] M.L. Sanz, M. Villamiel, I. Martínez-Castro, Food Chem. 87 (2004) 325–328.
[17] H.C. Bold, Bull. Torrey Bot. Club 76 (1949) 101–108.
[18] M. Zhou, H. He, T. Jin, H. Wang, J. Power Sources 214 (2012) 216–219.
[19] A.L. Lehninger, Bioenergetics: The Molecular Basis of Biological Energy Transformations. W.A. Benjamin Inc., California, 1971.
[20] APHA, AWWA, WPFC, Standard Methods for Examination of Water and Wastewater, twentieth ed., American Public Health Association, Washington, DC, 1998.
[21] R.P. Ramasamy, Z. Ren, M.M. Meneh, J.M. Regan, Biotechnol. Bioeng. 101 (2008) 101–108.
[22] M. Behera, M.M. Ghangrekar, Bioresour. Technol. 100 (2009) 5114–5121.
[23] B.H. Sorensen, N. Nyholm, A. Baun, Chemosphere 32 (1996) 1513–15521.
[24] J.W. Rachlin, A. Grosso, Arch. Environ. Contam. Toxicol. 20 (1991) 505–508.
[25] B.E. Logan, Microbial Fuel Cells, John Wiley & Sons, New Jersey, 2008.
[26] K.B. Cantrell, T. Ducey, K.S. Ro, P.G. Hunt, Bioresour. Technol. 99 (2008) 7941–7953.
[27] Y. Ahn, B.E. Logan, Bioresour. Technol. 101 (2010) 469–475.
[28] D.P.B.T.B. Strik, H.V.M. Hamelers, C.J.N. Buisman, Environ. Sci. Technol. 44 (2010) 532–537.
[29] M.A. Rodrigo, P. Cañizares, J. Lobato, Bioresour. Technol. 101 (2010) 7014–7018, 4710.
[30] G.H. Kim, H.S. Park, H.J. Kim, G.T. Kim, J.L. Chang, N.T. Phung, Appl. Microbiol. Biotechnol. 63 (2004) 672–681.
[31] D.R. Bond, D.R. Lovley, Appl. Environ. Microbiol. 69 (2003) 1548–1555.
[32] S.K. Chaudhuri, D.R. Lovley, Nat. Biotechnol. 21 (2003) 1229–1232.
[33] K. Raman, J.C.-W. Lan, Appl. Energy 100 (2012) 100–105.
[34] C. Wu, X.W. Liu, W.W. Li, G.P. Sheng, G.L. Zang, Y.Y. Cheng, N. Shen, Y.P. Yang, H.Q. Yu, Appl. Energy 98 (2012) 594–596.
[35] I. Ieropoulos, J. Greenman, C. Melhuish, Int. J. Energy Res. 32 (2008) 1228–1240.
[36] M.E. Orazem, P. Shukla, M.A. Membrino, Eletrochim. Acta 47 (2002) 2027–2034.
[37] A.P. Borole, D. Aaron, C.Y. Hamilton, C. Tsouris, Environ. Sci. Technol. 44 (2010) 2740–2745.
[38] Z. Ren, H. Yan, W. Wang, M.M. Mench, J.M. Regan, Environ. Sci. Technol. 45 (2011) 2435–2441.
[39] A.K. Manohar, O. Bretschger, K.H. Nealson, F. Mansfeld, Bioelectrochemistry 72 (2008) 149–154.
[40] E. Martin, O. Savadogo, S.R. Guiot, B. Tartakovsky, J. Appl. Electrochem. 43 (2013) 533–540.